The Role of Haptotropic Shifts in Phosphine Addition to Tricarbonylmanganese Organometallic Complexes: The Indenyl Effect Revisited†

Luis F. Veiros‡

Centro de Química Estrutural, Instituto Superior Técnico, 1049-001 Lisboa, Portugal

Received February 29, 2000

The addition of PH_3 to $[(\eta^5\text{-X})Mn(CO)_3]$ was studied by means of molecular orbital calculations performed with the B3LYP HF/DFT hybrid functional. Five reactions, with different π ligands, were compared: X = cyclopentadienyl (Cp = $C_5H_5^-$), indenyl (Ind = $C_9H_7^-$), fluorenyl (Flu = $C_{13}H_9^-$), cyclohexadienyl (Chd = $C_6H_7^-$), and 1-hydronaphthalene (Hnaph = $C_{10}H_9^-$). In each case, the optimized structures obtained for the η^5 complexes are compared with the corresponding experimental X-ray structures and the $(\eta^5\text{-X})-Mn$ bonding is discussed. The results show a η^5 coordination geometry in all cases, with a weakening of the polyenyl bonding with the increase of the corresponding π system extension, for Cp, Ind, and Flu. The cyclohexadienyl bonding to the metal proved to be comparable to the indenyl one, and the $(\eta^5\text{-Hnaph})-Mn$ bond is the weaker of the series. The electronic structure of the reaction products, $[(\eta\text{-X})Mn(CO)_3(PH_3)]$, was analyzed, and the corresponding optimized geometries were obtained. With the exception of Cp, all the remaining species present a η^3 coordination geometry for the polyenyl ligand, X. Folded η^3-X were found for Ind, Chd, and Hnaph, and an exocyclic allylic coordination is present in $[(\eta^3\text{-Flu})Mn(CO)_3(PH_3)]$. The cyclopentadienyl species has a slipped Cp with a η^2 coordination geometry, due to the destabilization associated with the folding of the Cp. The transition states of each of the five reactions were identified, and all present X coordination geometries close to the products. The obtained activation energies indicate the following order for the reaction rates: Cp ≪ Ind ≈ Chd < Flu < Hnaph, which correlates with the $(\eta^5\text{-X})-Mn$ bond strength in the reactants.

Introduction

An increase of the electron count on the metal center is a process known to induce ring slippage on π ligand complexes.[1] This can be accomplished by electrochemical reduction or by ligand addition. The geometric rearrangement involved in the haptotropic shift plays an important role in substitution reactions proceeding by associative mechanisms, the reaction rate being often related with the ease of the haptotropic shift. Basolo et al. studied the kinetics of phosphine substitution on tricarbonylmanganese complexes, $[(\eta^5\text{-X})Mn(CO)_3]$, and found[2] a remarkable increase in the reaction rate for indenyl complexes (X = Ind = $C_9H_7^-$) when compared with their cyclopentadienyl analogues (X = Cp = $C_5H_5^-$), coining the term *indenyl effect* to describe it. The rate enhancement increases with the ligand's π system extension, as shown by studies with fluorenyl complexes (X = Flu = $C_{13}H_9^-$),[3] being directly related with the stability of the lower hapticipty intermediates, normally η^3-X species. However, the opposite was found[4] for ligand substitution on 19-electron centers, resulting from the reduction of $[(\eta^5\text{-X})Fe(CO)_3]^+$ (X = Cp and Ind). In this case, a reverse indenyl effect occurs.

Since Basolo's early studies, the indenyl effect was proved to be present in a number of catalytic reactions,[5−11] the η^5 to η^3 ring slippage of the cyclic polyenic ligand playing an important role in the reaction mechanism. Normally, the lower hapticipty intermediates are unstable species and are hard to isolate and characterize, in most cases being only postulated. Given the general importance of those reactions, considerable interest as been devoted to the study and characterization of organometallic complexes with slipped or folded polyenic ligands, to serve as models for unstable intermediates. A variety of ligands and coordination modes have been covered, as shown by a Cambridge Structural Data Base (CSD)[12] survey.

Even for Cp, η^5 to η^3 shifts have been reported, with the η^3-Cp complexes characterized in solution[13] or in the

† Dedicated to Professor Alberto Romão Dias.

‡ E-mail: veiros@ist.utl.pt.

(1) O'Connor, J. M.; Casey, C. P. *Chem. Rev.* **1987**, *87*, 307.
(2) Rerek, M. E.; Ji, L.-N.; Basolo, F. *J. Chem. Soc., Chem. Commun.* **1983**, 1208.
(3) Ji, L.-N.; Rerek, M. E.; Basolo, F. *Organometallics* **1984**, *3*, 740.
(4) Pevear, K. A.; Banaszak Holl, M. M.; Carpenter, G. B.; Rieger, A. L.; Rieger, P. H.; Sweigart, D. A. *Organometallics* **1995**, *14*, 512.
(5) Marder, T. B.; Roe, D. C.; Milstein, D. *Organometallics* **1988**, *7*, 1451.
(6) Borrini, A.; Diversi, P.; Ingrosso, G.; Lucherini, A.; Serra, G. *J. Mol. Catal.* **1985**, *30*, 181.
(7) Bönnemann, H. *Angew. Chem., Int. Ed. Engl.* **1985**, *24*, 248.
(8) Foo, T.; Bergman, R. G. *Organometallics* **1992**, *11*, 1801.
(9) Schmid, M. A.; Alt, H. G.; Milius, W. *J. Organomet. Chem.* **1996**, *514*, 45.
(10) Llinas, G. H.; Day, R. O.; Rausch, M. D.; Chien, J. C. W. *Organometallics* **1993**, *12*, 1283.
(11) Garrett, C. E.; Fu, G. C. *J. Org. Chem.* **1998**, *63*, 1370.
(12) Allen, F. H.; Davies, J. E.; Galloy, J. J.; Johnson, O.; Kennard, O.; Macrae, C. F.; Watson, D. G. *J. Chem. Inf. Comput. Sci.* **1991**, *31*, 204.

10.1021/om000195j CCC: $19.00
Publication on Web 07/11/2000

solid state.[14] However, the more largely studied ligand is indenyl, a number of η^3-indenyl derivatives being characterized, detected, or simply postulated as intermediates in several substitution reactions.[15−23] Electrochemical reduction[24−30] or ligand addition[31] was shown to induce the η^5 to η^3 haptotropic shifts. NMR results are often[32−36] used to determine the indenyl coordination mode, a systematization of the different geometries and the development of the corresponding parameters being done by Habib et al.[37]

For ligands with large π systems, such as fluorenyl or cyclopenta[*def*]phenantrenyl, an η^3 exocyclic coordination mode is proposed,[16,38−41] since the presence of a rigid C_5 ring prevents a folded geometry. However, full structural characterizations are only available for some fluorenyl complexes.[42−44]

The theoretical understanding of haptotropic shifts and bonding in the different coordination geometries of polyenic ligands started with the pioneer work by Hoffmann et al.[45] Since then, a large amount of work has appeared, mostly dealing with Cp and Ind complexes, studying the ligand bonding in the different possible hapticities[46−51] or specifically addressing the indenyl effect.[26−28,31,52,53] The η^3 coordination mode in fluorenyl and cyclopenta[*def*]phenantrenyl complexes has also been the subject of theoretical work.[40,41,44] Recently, a comparative study was published of the η^5 to η^3 ring slippage resulting from the reduction of [(η^5-X)Mn(CO)$_3$] complexes with a series of π ligands.[54]

The electronic structure of the cyclohexadienyl ligand (X = Chd = $C_6H_7^-$) and its coordination geometry in [(η^5-C_6H_7)Fe(CO)$_3$]$^+$ was first studied by Hoffmann et al.[55] and later complemented with a study on the reactivity of this complex toward nucleofic addition to the dienyl.[56] But, to our knowledge, η^5 to η^3 haptotropic shifts of cyclohexadienyl complexes have never been the subject of theoretical work. Also the bonding of η^3-$C_6H_7^-$ in a transition metal complex has not been studied, despite its appearance in numerous postulated reaction intermediates.[57−63] On the other hand, a η^3-1-hydronaphthalene (X = Hnaph = $C_{10}H_9^-$) complex, [(η^3-$C_{10}H_9$)Mn(CO)$_3$P(OCH$_3$)$_3$], has been recently synthesized[64] and later structurally characterized by X-ray diffraction.[65]

This work reports a comparative study of the phosphine addition to tricarbonylmanganese complexes with a series of π ligands. Five ligands were chosen (see Scheme 1), three of which bond to the metal through a C_5 pentagonal ring, when η^5 coordinated, X = Cp, Ind, and Flu. The other two, cyclohexadienyl and 1-hydronaphthalene, achieve η^5 coordination through five

(13) Simanko, W.; Sapunov, V. N.; Schmid, R.; Kirchner, K.; Wherland, S. *Organometallics* **1998**, *17*, 2391.
(14) Huttner, G.; Britzinger, H. H.; Bell, L. G.; Frieddrich, P.; Bejenke, V.; Neugebauer, D. *J. Organomet. Chem.* **1978**, *141*, 329.
(15) Kowalewski, R. M.; Rheingold, A. L.; Trogler, W. C.; Basolo, F. *J. Am. Chem. Soc.* **1986**, *108*, 2460.
(16) Zhou, Z.; Jablonski, C.; Brisdon, J. *J. Organomet. Chem.* **1993**, *461*, 215.
(17) Biagioni, R. N.; Luna, A. D.; Murphy, J. L. *J. Organomet. Chem.* **1994**, *476*, 183.
(18) Brown, D. A.; Fitzpatrick, N. J.; Glass, W. K.; Ahmed, H. A.; Cunningham, D.; McArdle, P. *J. Organomet. Chem.* **1993**, *455*, 157.
(19) Merola, J. S.; Kacmarcik, R. T.; Van Engen, D. *J. Am. Chem. Soc.* **1986**, *108*, 329.
(20) Forschner, T. C.; Cutler, A. R.; Kullnig, R. K. *Organometallics* **1987**, *6*, 889.
(21) Poli, R.; Mattamana, S. P.; Falvello, L. R. *Gazz. Chim. Ital.* **1992**, *122*, 315.
(22) Ascenso, J. R.; Azevedo, C. G.; Gonçalves, I. S.; Herdtweck, E.; Moreno, D. S.; Romão, C. C.; Zühlke, J. *Organometallics* **1994**, *13*, 429.
(23) Gonçalves, I. S.; Romão, C. C. *J. Organomet. Chem.* **1995**, *486*, 155.
(24) Miller, G. A.; Therien, M. J.; Trogler, W. C. *J. Organomet. Chem.* **1990**, *383*, 271.
(25) Ascenso, J. R.; Azevedo, C. G.; Gonçalves, I. S.; Herdtweck, E.; Moreno, D. S.; Pessanha, M.; Romão, C. C. *Organometallics* **1995**, *14*, 3901.
(26) Calhorda, M. J.; Gamelas, C. A.; Romão C. C.; Veiros, L. F. *Eur. J. Inorg. Chem.* **2000**, 331.
(27) Calhorda, M. J.; Gamelas, C. A.; Gonçalves, I. S.; Herdtweck, E.; Lopes, J. P.; Romão, C. C.; Veiros, L. F. *XIIth* FECHEM, Prague, Tcheck Republic, 1997.
(28) Calhorda, M. J.; Félix, V.; Gamelas, C. A.; Gonçalves, I. S.; Romão, C. C.; Veiros, L. F. XVII Reunión del Grupo Especializado de Química Organometálica, Barcelona, Spain, 1998.
(29) Lee, S.; Lovelace, S. R.; Cooper, N. J. *Organometallics* **1995**, *14*, 1974.
(30) Amatore, C.; Ceccon, A.; Santi, S.; Verpeaux, J.-N. *Chem. Eur. J.* **1997**, *3/2*, 279.
(31) Calhorda, M. J.; Gamelas, C. A.; Gonçalves, I. S.; Herdtweck, E.; Romão, C. C.; Veiros, L. F. *Organometallics* **1998**, *17*, 2597.
(32) Huber, T. A.; Bélanger-Gariépy, F.; Zargarian, D. *Organometallics* **1995**, *14*, 4997.
(33) Huber, T. A.; Bayrakdarian, M.; Dion, S.; Dubuc, I.; Bélanger-Gariépy, F.; Zargarian, D. *Organometallics* **1997**, *16*, 5811.
(34) Crabtree, R. H.; Panell, C. P. *Organometallics* **1984**, *3*, 1727.
(35) Marder, T. B.; Calabrese, J. C.; Roe, D. C.; Tulip, T. H. *Organometallics* **1987**, *6*, 2012.
(36) Faller, J. W.; Chen, C.-C.; Mattina, M. J.; Jakubowski, A. *J. Organomet. Chem.* **1973**, *52*, 361.
(37) Faller, J. W.; Crabtree, R. H.; Habib, A. *Organometallics* **1985**, *4*, 929.
(38) Biagioni, R. N.; Lorkovic, I. M.; Skelton, J.; Hartung, J. B. *Organometallics* **1990**, *9*, 547.
(39) Rerek, M. E.; Basolo, F. *Organometallics* **1984**, *3*, 647.
(40) Decken, A.; Britten, J. F.; McGlinchey, M. J. *J. Am. Chem. Soc.* **1993**, *115*, 7275.
(41) Decken, A.; Rigby, S. S.; Girard, L.; Bain, A. D.; McGlinchey, M. J. *Organometallics* **1997**, *16*, 1308.
(42) Diamond, G. M.; Green, M. L. H.; Mountford, P.; Popham, N. A.; Chernega, A. N. *J. Chem. Soc., Chem. Commun.* **1994**, 103.
(43) Bochmann, M.; Lancaster, S. J.; Hursthouse, M. B.; Mazid, M. *Organometallics* **1993**, *12*, 4718.
(44) Calhorda, M. J.; Gonçalves, I. S.; Herdtweck, E.; Romão, C. C.; Royo, B.; Veiros, L. F. *Organometallics* **1999**, *18*, 3956.
(45) Albright, T. A.; Hofmann, P.; Hoffmann, R.; Lillya, C. P.; Dobosh, P. A. *J. Am. Chem. Soc.* **1983**, *105*, 3396.
(46) Kakkar, A. K.; Taylor, N. J.; Calabrese, J. C.; Nugent, W. A.; Roe, D. C.; Connaway, E. A.; Marder, T. B. *J. Chem. Soc., Chem Commun.* **1989**, 990.
(47) O'Hare, D.; Green, J. C.; Marder, T. B.; Collins, S.; Stringer, G.; Kakkar, A. K.; Kaltsoyannis, N.; Kuhn, A.; Lewis, R.; Mehnert, C.; Scott, P.; Kurmoo, M.; Pugh, S. *Organometallics* **1992**, *11*, 48.
(48) Crossley, N. S.; Green, J. C.; Nagy, A.; Stringer, G. *J. Chem. Soc., Dalton Trans.* **1989**, 2139.
(49) Frankcom, T. M.; Green, J. C.; Nagy, A.; Kakkar, A. K.; Marder, T. B. *Organometallics* **1993**, *12*, 3688.
(50) Green, J. C.; Parkin, R. P. G.; Yang, X.; Haaland, A.; Scherer, W.; Tapifolsky, M. *J. Chem. Soc., Dalton Trans.* **1997**, 3219.
(51) Field, C. N.; Green, J. C.; Moody, A. G. J.; Siggel, M. R. F. *Chem. Phys.* **1996**, *206*, 211.
(52) Bonifaci, C.; Ceccon, A.; Santi, S.; Mealli, C.; Zoellner, R. W. *Inorg. Chim. Acta* **1995**, *240*, 541.
(53) Calhorda, M. J.; Veiros, L. F. *Coord. Chem. Rev.* **1999**, *185−186*, 37.
(54) Veiros, L. F. *J. Organomet. Chem.* **1999**, *587*, 221.
(55) Hoffmann, R.; Hofmann, P. *J. Am. Chem. Soc.* **1976**, *98*, 598.
(56) Eisenstein, O.; Butler, W. M.; Pearson, A. J. *Organometallics* **1984**, *3*, 1150.
(57) Pearson, A. J. *Metallo-Organic Chemistry*; J. Wiley: Chichester, 1988.
(58) Carvalho, M. F. N. N.; Pombeiro, A. J. L.; Shrophire, I. M.; Stephenson, G. R. *Inorg. Chim. Acta* **1996**, *248*, 45.
(59) Lehmann, R. E.; Kochi, J. K.; *Organometallics* **1991**, *10*, 190.
(60) Kreiter, C. G.; Fiedler, C.; Frank, W.; Reiss, G. J *J. Organomet. Chem.* **1995**, *490*, 133.
(61) Verona, I.; Gutheil, J. P.; Pike, R. D.; Carpenter, G. B. *J. Organomet. Chem.* **1996**, *524*, 71.
(62) Zhang, X.; Dullaghan, C. A.; Watson, E. J.; Carpenter, G. B.; Sweigart, D. A. *Organometallics* **1998**, *17*, 2067.
(63) Balssa, F.; Gagliardini, V.; Rose-Munch, F.; Rose, E. *Organometallics* **1996**, *15*, 4373.
(64) Georg, A.; Kreiter, C. G. *Eur. J. Inorg. Chem.* **1999**, 651.
(65) Son, S. U.; Paik, S.-J.; Lee, I. S.; Lee, Y.-A.; Chung, Y. K.; Seok, W. K.; Lee, H. N. *Organometallics* **1999**, *18*, 4114.

Scheme 1

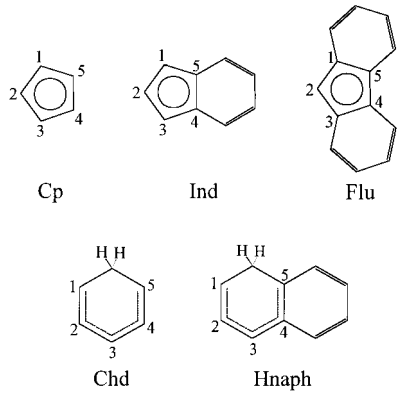

carbon atoms of a hexagonal C_6 ring, the sixth atom being a saturated methylene carbon.

The studied reaction (eq 1) corresponds to the first step of a substitution reaction proceeding through an associative mechanism, such as the one originally proposed by Basolo, X = Cp, Ind,[2] Flu,[3] and C_5Me_5.[66] Addition of the phosphine to an 18-electron complex induces the η^5 to η^3 haptotropic shift, to avoid an unstable 20-electron species.

$$PH_3 + [(\eta^5\text{-X})Mn(CO)_3] \rightarrow [(\eta^3\text{-X})Mn(CO)_3(PH_3)] \quad (1)$$

This reaction is studied by means of ab initio[67] and DFT[68] molecular orbital calculations, complemented with the orbital analysis provided by the extended Hückel method.[69,70] The optimized geometries of the reactants and products are compared with experimental X-ray structures, when available,[12] i.e., all η^5 species and the X = Hnaph product; the results are used to test the theoretical model. The electronic structure and the bonding of the polyenyl ligand to the metal are analyzed in all species and in the corresponding transition states.

Results and Discussion

The bonding of the polyenyl ligands, X, in the η^5 species is qualitatively similar for all the studied complexes and has been studied for the two ligand geometries: Cp and its derivatives, bonding to the metal through a pentagonal C_5 ring;[54] and Chd,[55,56] in which five carbon atoms out of a C_6 ring establish the bond. Figure 1 has a simplified, schematic representation of the $(\eta^5$-X)−Mn bonding for the five $[(\eta^5$-X)$Mn(CO)_3]$ complexes, with the notation used in the following discussion. The overall Mn−X bond is based on three interactions. One, of σ symmetry, involves an empty metal *z* orbital and a filled symmetrical ligand π orbital (π_σ in Figure 1), which is usually the more stable of the π set. The remaining two are π bonds, resulting from the interaction between the two empty metal d orbitals (*yz* and *xz*) pointing toward X, and the ligand-filled π orbitals with appropriate symmetry ($\pi_{||}$ and $\pi_\perp$). The result is the formation of three filled bonding molecular orbitals, σ, $\pi_{||}$, and $\pi_\perp$, and the corresponding empty antibonding counterparts, i.e., the net formation of three X−Mn bonds, that formally can be viewed as three two-electron donations from the ligand to the metal. Of the filled metal d orbitals, two are parallel to the ligand X plane, *xy* and x^2-y^2; these have no significant overlap with the ligand orbitals and remain practically nonbonding. There is a small mixture of metal z^2 into the σ interaction, slightly destabilizing that orbital, which becomes the highest occupied molecular orbital (HOMO) of the species.

The geometrical parameters used to characterize the polyenyl ligands hapticipty throughout this work are depicted in Scheme 2, for two representative examples, X = Ind and Hnaph. Two criteria are used, of all defined for Ind:[37] the five Mn−C distances and the folding angle, Ω. This is the angle between the planes of the two halves of a folded η^3-X ligand, i.e., the angle between the plane of C1, C2, and C3, and the mean plane of C1, C3, C4, and C5 (Scheme 2), for all X ligands but Flu. For this ligand, the presence of the two fused benzene rings prevents the bending of the C_5 bonded pentagon in the η^3 coordination mode.

The optimized structures obtained for the studied compounds are represented in Figure 2. Due to computational limitations, the geometry optimizations were performed with the smallest all-electron basis set known to yield reasonable geometries.[67] Nevertheless, the adopted theoretical model (see Computational Details) was tested through the comparison of the obtained geometrical parameters with the corresponding experimental values, for all the species with X-ray determinations, i.e., all the reactants, $[(\eta^5$-X)$Mn(CO)_3]$, and the X = Hnaph product. The results are compiled in Table 1 for the structural parameters more relevant to the following discussion, namely, the bonding distances of the metal coordination sphere and the folding angle, Ω. Thus, both the mean (δ) as well as the maximum (Δ) absolute deviations are presented in Table 1, for each type of bond, Mn−C(X), Mn−C(CO), and C−O. These are calculated as the absolute value of the difference between the optimized and the experimental value for the corresponding bond length ($|d_{opt} - d_{exp}|$).

The even distribution shown by the tabulated values, both for the same bond of all the complexes as well as for the different bonds, gives a good indication of the method consistency. In fact, there are no discrepancies for the same type of bond, and, on the other hand, none of the bonds are significantly worse described by the used theoretical model. The obtained deviation values for the bond distances, 0.007 Å < δ < 0.028 Å, and 0.009 Å < Δ < 0.053 Å, and for the folding angles, 0° < Δ_Ω < 5° ($\Delta_\Omega = |\Omega_{opt} - \Omega_{exp}|$), although not perfect, are completely suitable for the structural discussion here intended, providing, thus, a solid support for the performance of the theoretical approach used for the description of the studied systems. This is especially noticeable since three out of the six available[12] experimental X-ray structures, presented in Table 1, do not correspond exactly to the studied complexes, namely, the X = Ind[72] and Flu[73] η^5 complexes and the X =

(66) Rerek, M. E.; Basolo, F. *Organometallics* **1983**, *2*, 372.
(67) Hehre, W. J.; Radom, L.; Schleyer, P. v. R.; Pople, J. A. *Ab Initio Molecular Orbital Theory*; John Wiley & Sons: New York, 1986.
(68) Parr, R. G.; Yang, W. *Density Functional Theory of Atoms and Molecules*; Oxford University Press: New York, 1989.
(69) Hoffmann, R. *J. Chem. Phys.* **1963**, *39*, 1397.
(70) Hoffmann, R.; Lipscomb, W. N. *J. Chem. Phys.* **1962**, *36*, 2179.
(71) Cowie, J.; Hamilton, E. J. M.; Laurie, J. C. V.; Welch, A. J. *J. Organomet. Chem.* **1990**, *394*, 1.
(72) Honan, M. B.; Atwood, J. L.; Bernal, I.; Herrmann, W. A. *J. Organomet. Chem.* **1979**, *179*, 403.

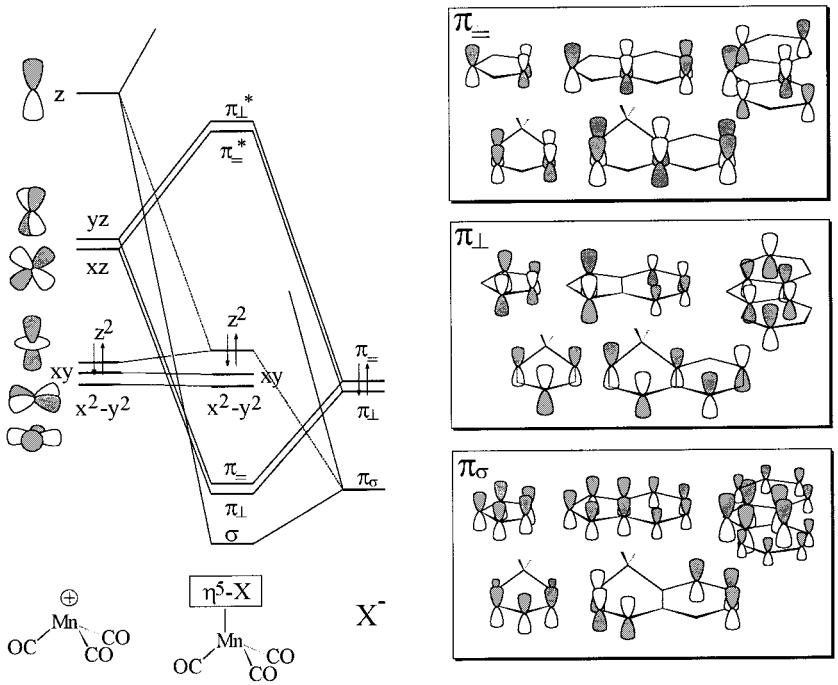

Figure 1. Simplified schematic MO diagram for the $(\eta^5\text{-X})^-$−$[Mn(CO)_3]^+$ bonding (X = Cp, Ind, Flu, Chd, and Hnaph).

Scheme 2

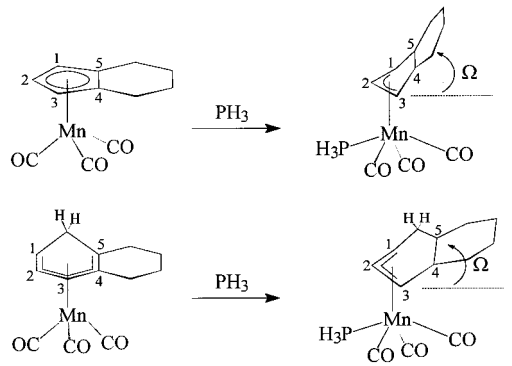

Hnaph η^3 product, $[(\eta^3\text{-}C_{10}H_9)Mn(CO)_3P(OCH_3)_3]$.[65] The first two have substituted X ligands, X = BrInd (Br bonded to C1) and X = PhFlu (phenyl group bonded to C2); and the η^3 complex has a phosphite, $P(OCH_3)_3$, coordinated instead of the simple PH_3 used in the calculations. In these cases a perfect match between the calculated and the experimental geometrical parameters could never be expected.

All reactants, $[(\eta^5\text{-X})Mn(CO)_3]$, present piano stool geometries with clear η^5 coordination of the polyenyl ligands, X, small distortions from a perfect η^5-X being found for all but the 1-hydronaphthalene complex, as shown by the short range obtained for the five Mn−C bonding distances, 2.121 Å < d_{Mn-C} < 2.237 Å, and the folding angles Ω < 5° (see Figure 2). On the other hand, $[(\eta^5\text{-Hnaph})Mn(CO)_3]$ presents a quite folded polyenyl ligand, as shown by the folding angle, Ω = 18°, and by the two long Mn−C distances (d_{Mn-C4} = 2.280 Å and d_{Mn-C5} = 2.394 Å). In fact, "$\eta^3 + \eta^2$" is a better designation for the Hnaph coordination, as previously[53] proposed for some indenyl complexes.

Another important aspect of the coordination geometry for X = Chd and Hnaph is the methylene out of plane bending. This feature was proven to be the result of a repulsive interaction between the metal and the CH_2 hydrogen for $[(\eta^5\text{-Chd})M(CO)_3]$ complexes,[55] being, thus, closely related to the $(\eta^5\text{-X})$−M bonding. A good concordance is found between the experimental values and the ones obtained for the optimized structures, 44° and 42° for Chd, 42° and 35° for Hnaph, respectively.

The bonding in the metallic fragment $[Mn(CO)_3]$ is very similar in all η^5 species with very narrow ranges for the values obtained for the Mn−C(CO) and C−O bond distances, 1.766−1.796 and 1.171−1.173 Å, respectively.

The addition of a two-electron donor such as PH_3 to an 18-electron complex with a η^5 coordinated π ligand, X, is expected to induce a η^5 to η^3 haptotropic shift, as the presence of two extra electrons on an electronic saturated metal center will force the breaking of two M−C bonds. The final coordination geometry of the η^3-X ligand results from the balance between electronic factors and van der Waals interligand repulsive and attractive interactions. This is what happens with the solvolysis of $[(\eta^5\text{-Ind})Mo(CO)_2(MeCN)_2]^+$ in acetonitrile, yielding the structurally characterized $[(\eta^3\text{-Ind})Mo(CO)_2(MeCN)_3]^+$, the process being thoroughly studied from the theoretical point of view.[31] In fact, the two extra electrons added by the incoming phosphine to the metal center of a $[(\eta^5\text{-X})Mn(CO)_3]$ complex has the same effect; that is, it will force the occupation of a X−Mn antibonding orbital, $\pi_{||}$* (see Figure 1), the stabilization of this orbital being the driving force of the geometrical distortion associated with the haptotropic shift. This is clear in Figure 3 representations, in which the addition of a PH_3 to $[(\eta^5\text{-Ind})Mn(CO)_3]$ is shown to result in the occupation of this complex's lowest unoccupied molecular orbital (LUMO), $\pi_{||}$*, which is further stabilized by the indenyl ring folding, i.e., the augmentation of the two Mn−$C_{4/5}$ distances. Figure 3 orbitals correspond to

(73) Reference taken from the CSD: Yarmolenko, A. I.; Kukharenko, S. V.; Novikova, L. N.; Ustynyuk, N. A.; Dolgushin, F. M.; Yanovsky, A. I.; Struchkov, Yu. T.; Kaftaeva, T. G.; Oprunenko, Yu. F.; Strelets, V. V. *Izv. Akad. Nauk SSSR, Ser. Khim.* **1996**, 199.

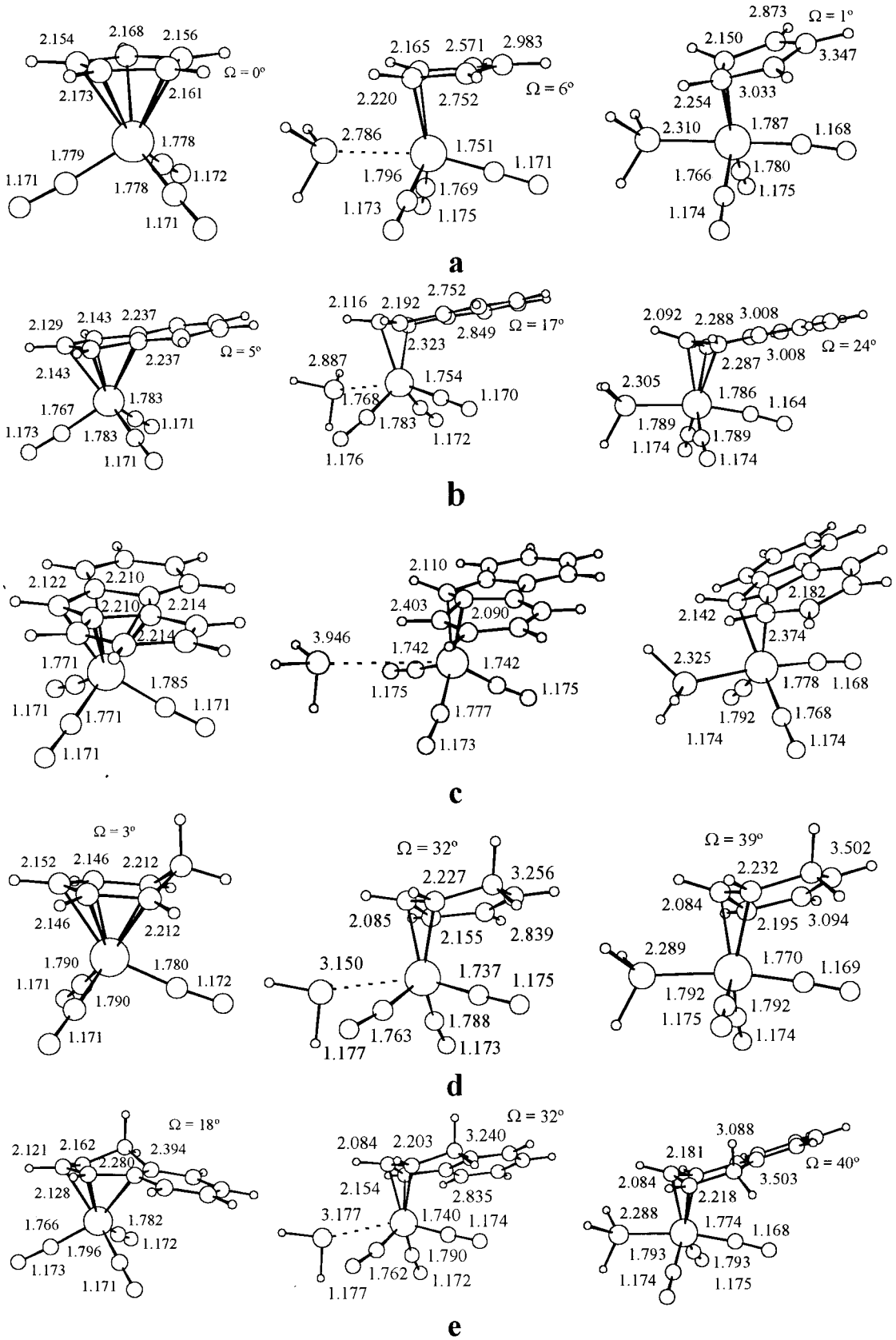

Figure 2. Optimized geometries (B3LYP/3-21G(*)) and more relevant geometrical parameters (distances in Å) for [(η^5-X)Mn(CO)$_3$] (left), the phosphine adducts, [(η-X)Mn(CO)$_3$(PH$_3$)] (right), and the corresponding transition states (center); X = Cp (a), Ind (b), Flu (c), Chd (d), and Hnaph (e).

models with C_s symmetry, to diminish orbital mixing and enhance clarity.

The optimized structures of Figure 2 show that three of the studied complexes present clearly folded geometries for the η^3 coordination of the corresponding π ligands, X, in the phosphine adducts: X = Ind, Chd, and Hnaph. This is shown by the corresponding folding angles, Ω = 24° (X = Ind), 39° (X = Chd), and 40° (X =

Table 1. Mean (δ) and Maximum (Δ) Absolute Deviations[a] for Relevant Geometrical Parameters of the Optimized Structures and the Corresponding Available[12] X-ray Structures (Distances in Å and Angles in deg)

	Mn−C(X)		Mn−C(CO)		C−O		Mn−P	Ω	
	δ	Δ	δ	Δ	δ	Δ	Δ	Δ_Ω	ref
[(η^5-X)Mn(CO)$_3$]									
X = Cp	0.024	0.032	0.018	0.019	0.013	0.020		0	71
X = BrInd[b]	0.017	0.032	0.016	0.034	0.028	0.041		1	72
X = PhFlu[b]	0.015	0.032	0.022	0.031	0.021	0.029			73
X = Chd	0.007	0.011	0.007	0.009	0.015	0.018		1	74
X = Hnaph	0.016	0.035	0.011	0.019	0.026	0.028		1	75
[(η^3-Hnaph)Mn(CO)$_3$P(OMe)$_3$][b]	0.028	0.053	0.017	0.052	0.026	0.028	0.044	5	65

[a] $\delta = (\sum|d_{opt} - d_{exp|i})/N$; $\Delta = \max\{|d_{opt} - d_{exp}|\}$; $\Delta_\Omega = |\Omega_{opt} - \Omega_{exp}|$. [b] Experimental structures only available for modified complexes.

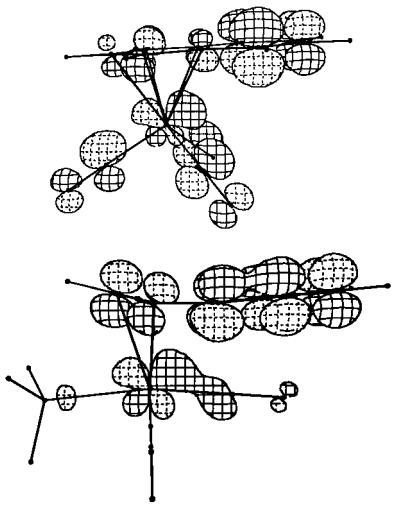

Figure 3. 3D representations of the [(η^5-Ind)Mn(CO)$_3$] LUMO (top) and the [(η^3-Ind)Mn(CO)$_3$(PH$_3$)] HOMO (bottom).

Hnaph), as well as by the breaking of two of the Mn−C(X) bonds. In fact, in these [(η^3-X)Mn(CO)$_3$(PH$_3$)] complexes, three of the Mn−C distances remain within bonding distances, $2.084 < d_{Mn-Cx} < 2.288$ Å ($x = 1, 2, 3$), while the other two carbon atoms are pushed away from the metal, $3.008 < d_{Mn-Cx} < 3.503$ Å ($x = 4, 5$).

The coordination geometry around the metal can be viewed as pseudo-octahedral, as expected for a d^6 metal center, in which the η^3-X ligand occupies two adjacent positions. If we take this as the equatorial plane, for discussion sake, then the entering phosphine remains in the apical position opposite the folded X ligand in all complexes (see Figure 2). This choice of coordination position is not fortuitous, being the result of both electronic and stereochemical reasons, as already pointed out in the P(OMe)$_3$ addition to [(η^5-Hnaph)Mn(CO)$_3$], yielding [(η^3-Hnaph)Mn(CO)$_3$P(OMe)$_3$].[64] Thus, of the four available coordination positions for the incoming phosphine, electronic reasons force the occupation of one apical site, since this is the only way to avoid the presence of two trans carbonyl ligands, that is, two strong π acceptors competing for the same metal orbitals. On the other hand, from the two apical possibilities, the less crowded one, from the stereochemical point of view, is chosen, i.e., the one opposite the folded η^3-X ligand.

The bonding in the metallic fragment, [Mn(CO)$_3$(PH$_3$)], is very similar in the three [(η^3-X)Mn(CO)$_3$(PH$_3$)] complexes (X = Ind, Chd, and Hnaph), the bond lengths being within short ranges, $1.770 < d_{Mn-C(CO)} < 1.793$ Å, $1.164 < d_{C-O} < 1.175$ Å, and $2.288 < d_{Mn-P} < 2.305$, as well as the angles in the metal coordination sphere, 169° < PH$_3$−Mn−CO(ap) < 170° and 110° < CO(eq)−Mn−CO(eq) < 112°. These show some deviation from the values of a perfect octahedron, 180° and 90°, as expected for the studied complexes, with different ligands and a η^3-X occupying two adjacent coordination positions.

Scheme 3

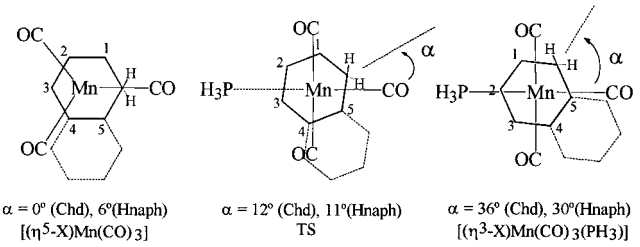

The electronic reasons behind the η^5 to η^3 haptotropic shift and the bonding in η^3-Ind complexes have been the subject of many works for other systems (see Introduction), and the parallel to the complexes here studied is straightforward, being unnecessary to repeat it. The same orbital reasoning used for the indenyl complex (see Figure 3) explains the η^5 to η^3 ring slippage present in the [(η^3-X)Mn(CO)$_3$(PH$_3$)] (X = Chd, Hnaph) complexes, i.e., the releasing of the antibonding character of the $\pi_{||}$* orbital that becomes occupied in the phosphine adducts. Nevertheless, there are some important differences for the cases of the two ligands binding through a C$_6$ ring, X = Chd and Hnaph, which are worth pointing out. The most significant of these differences is the stabilization of the folded X ligand and how it relates with the geometry of the η^3 coordinated ligand. In fact, the maintenance of a C_s or pseudo-C_s symmetry in an indenyl η^5 to η^3 ring slippage (see Scheme 2) has no parallel with the corresponding distortion of a cyclohexadienyl complex. The formation of a double bond between the two uncoordinating carbon atoms (C4 and C5) forces the rotation of the cyclohexadienyl with the consequent loss of a possible C_s symmetry present in the parent η^5-C$_6$H$_7$ complex. This rotation can be seen in the optimized geometries obtained for the X = Chd and Hnaph complexes, as well as in the corresponding X-ray structures,[65,74,75] and is schematically represented in Scheme 3. It can be measureed by the angle, α, defined by the projections of the Mn−C(CO) and Mn−C(CH$_2$) bonds, on the plane perpendicular to the one

(74) Churchill, M. R.; Scholer, F. R. *Inorg. Chem.* **1969**, *8*, 1950.
(75) Sun, S.; Dullaghan, C. A.; Carpenter, G. B.; Sweigart, D. A.; Lee, S. S.; Chung, Y. K. *Inorg. Chim. Acta* **1997**, *262*, 213.

defined by these two bonds (see Scheme 3). In the η^5 species the methylene carbon is close to eclipsing one of the CO ligands, $\alpha = 0°$ (Chd) and 6° (Hnaph), corresponding to a C_s or pseudo-C_s symmetry in the metal coordination sphere, which is broken in the η^3 phosphine adducts, where a significant rotation of the X ligand is found, $\alpha = 36°$ (Chd) and 30° (Hnaph). The transition states present intermediate distortions, $\alpha =$ 12° (Chd) and 11° (Hnaph). The stabilization of the folded η^3-X ligand is the driving force for the rotation, namely, the formation of an uncoordinated benzene ring in [(η^3-Hnaph)Mn(CO)$_3$(PH$_3$)] and of a C=C double bond between C4 and C5 in the Chd species, as shown be the C−C optimized distances, obtained for the [(η^3-Chd)-Mn(CO)$_3$(PH$_3$)] complex, the C4−C5 bond being much shorter (1.339 Å) than the remaining C−C bonds ($d_{C-C} > 1.4$ Å). The existence of an electronic reason behind this effect, instead of a stereochemically induced distortion, is proven by extended Hückel (EH) calculations performed with an ideal model with all C−C bond lengths equal to 1.4 Å (see Computational Details). In fact, the overlap population between C4 and C5 (1.175) well exceeds the values of the other C−C bonds: 0.843−1.056.

The phosphine adduct for the fluorenyl ligand, [(η^3-Flu)Mn(CO)$_3$(PH$_3$)], presents also an η^3 coordination of this ligand (see Figure 2). But, in this case, the two fused benzene rings create a rigid C_5 pentagon, preventing the folding of the ligand in a η^3 coordination mode. In fact, the result is an exocyclic allylic coordination, already found for the structurally characterized [(η^5-Ind)(η^3-Flu)Mo(CO)$_2$], resulting from the reduction of the parent dication complex, in which both π ligands bond to the metal in a η^5 mode.[44] Molecular orbital calculations have shown that the exocyclic geometry is the preferential one for the η^3 coordination of large X ligands, such as fluorenyl on the previous molybdenum complex,[44] as well as in the 2-electron reduction of [(η^5-X)Mn(CO)$_3$] with X = Flu[54] and cyclopenta[*def*]phenantrenyl,[41,54] which has three fused benzene rings.

The [(η^3-Flu)Mn(CO)$_3$(PH$_3$)] complex presents three fluorenyl carbon atoms within bonding distances from the metal, $2.142 < d_{Mn-C} < 2.374$ Å, establishing the η^3 coordination mode of the ligand. The geometry of the metallic portion is comparable to the ones found in the Ind, Chd, and Hnaph η^3 complexes, discussed above, with similar bond distances, $1.767 < d_{Mn-C(CO)} < 1.792$ Å, $1.168 < d_{C-O} < 1.174$ Å, $d_{Mn-P} = 2.325$ Å, and angles, PH$_3$−Mn−CO(ap) = 172°, CO(eq)−Mn−CO(eq) = 107°.

The adduct resulting from the phosphine addition to the Cp complex, [(η^5-Cp)Mn(CO)$_3$], presents a planar cyclopentadienyl ring ($\Omega = 1°$) with one C−C bond over the metal, instead of the expected folded η^3-Cp coordination. In fact, in the optimized geometry (Figure 2), there are two Mn−C(Cp) bonding distances, 2.150 and 2.254 Å, the other three carbon atoms being far away from the metal, $d_{Mn-C(Cp)} = 2.873$, 3.033, and 3.347 Å. This is achieved by an inclination of the Cp plane toward the plane defined by the metal and the two bonding carbon atoms (103°). This cyclopentadienyl coordination geometry, although unusual, is not new, being found before for triscyclopentadienyltitanium,[76] a complex with two ligands coordinating in the traditional η^5 way and the third binding through a C−C bond in a geometry identical to the one obtained here for [(η^2-Cp)-Mn(CO)$_3$(PH$_3$)]. The η^2-Cp ring has an inclination of 112° on the titanium complex, thus, comparable to the value obtained here for the phosphine adduct of the cyclopentadienyl complex. Another example of this type coordination in a related π ligand was found for an indenyl zirconium complex,[42] [{(CH$_2$)$_5$C(η^5-C$_5$H$_4$)(η^2-C$_9$H$_6$)}Zr(η^5-C$_5$H$_5$)Cl], in which the bite angle of a one carbon *ansa* bridge is forcing the indenyl coordination mode. On the other hand, the only folded η^3-Cp with an X-ray structure determination published so far belongs to a folded metallocene complex, [(η^5-Cp)(η^3-Cp)W(CO)$_2$],[14] not directly comparable with the species here studied. Interestingly, in the theoretically investigated two-electron reduction of [(η^5-Cp)Mn(CO)$_3$] a folded η^3-Cp geometry could not be found in the corresponding product,[54] which presents, instead, an almost planar η^1 coordinated cyclopentadienyl ring. However, in this case the optimization starting geometries and the C_s symmetry constraint used in the calculations would prevent the resulting reduced complex from presenting the η^2 coordination mode found in this work for [(η^2-Cp)Mn(CO)$_3$(PH$_3$)].

Extended Hückel calculations were performed on model complexes (see Computational Details) in order to understand the preferred η^2-Cp coordination geometry in the phosphine adduct and to compare it with a hypothetical folded cyclopentadienyl complex, [(η^3-Cp)-Mn(CO)$_3$(PH$_3$)]. The results yield a significantly more stable η^2 species with respect to the η^3 complex (by ca. 56 kcal/mol), with a stronger Cp−Mn bond, as shown by the corresponding overlap populations: 0.135 for (η^3-Cp)$^-$−[Mn(CO)$_3$(PH$_3$)]$^+$ and 0.304 for (η^2-Cp)$^-$−[Mn-(CO)$_3$(PH$_3$)]$^+$. In fact, on a folded η^3 coordination the Mn−Cp bonding is the result of three interactions, σ, $\pi_\perp$, and $\pi_\parallel$ (see Figure 1), yielding an occupied antibonding orbital ($\pi_\parallel$*), which is stabilized by the geometrical distortion, as discussed above for the X = Ind, Chd, and Hnaph complexes. On the other hand, for the η^2-Cp complex only two interactions are established (σ and $\pi_\perp$) and the filled metal *xz* orbital remains practically nonbonding, not being involved in the $\pi_\parallel$ interaction, avoiding the formation of a filled $\pi_\parallel$*. Thus, for [(η^5-Cp)-Mn(CO)$_3$], an increase of the metal electron count by two electrons is not expected to yield the corresponding η^3 species, as the destabilization corresponding to the folding of the cyclopentadienyl ligand and the consequent breaking of its aromaticity overtake the stabilization associated with the establishment of the third X−Mn interaction, $\pi_\parallel$, present in the η^3 complexes. These results corroborate well with the studies on the CO substitution by a phosphine in [(η^5-X)Mn(CO)$_3$] complexes (X = Cp, Ind, and Flu). The cyclopentadienyl complex does not react, while the reaction proceeds readily for the other two complexes, under the same conditions.[2] As these reactions proceed through an associative mechanism with a [(η^3-X)Mn(CO)$_3$(PH$_3$)] intermediate, an unstable η^3-Cp species will greatly impede, if not prevent, the process.

The bonding in the metallic fragment of [(η^2-Cp)Mn-(CO)$_3$(PH$_3$)] is equivalent to the ones found for the other phosphine adducts. The obtained bond lengths for the

(76) Lucas, C. R.; Green, M.; Forder, R. A.; Prout, K. *J. Chem. Soc., Chem. Commun.* **1973**, 97.

carbonyl ligands, $1.766 < d_{Mn-C(CO)} < 1.787$ Å and $1.168 < d_{C-O} < 1.175$ Å, as well as for the phosphine, $d_{Mn-P} = 2.310$ Å, are similar to the corresponding values of the η^3-X complexes. The same happens with the bonding angles in the metal coordination sphere, $PH_3-Mn-CO(ap) = 175°$ and $CO(eq)-Mn-CO(eq) = 101°$, showing that the different coordination mode of the π ligand, X, does not change significantly the metal electronic structure, the overall geometry remaining a distorted octahedron with the two bonding Cp carbon atoms occupying two adjacent positions.

All the optimized transition states (see Figure 2) present intermediate geometries between the initial η^5 complexes, [(η^5-X)Mn(CO)$_3$], and the phosphine adducts, [(η-X)Mn(CO)$_3$(PH$_3$)]. This can be seen in the values obtained for the rotation of the π ligand in the Chd and Hnaph transition states, $\alpha = 12°$ and 11°, respectively (cf. Scheme 3), and in the Mn−C(X) bonding distances, $2.084 < d_{Mn-C(X)} < 2.403$ Å, which are similar to the ones found for all the reactants and products. The same happens with the bonding in the metallic fragment, [Mn(CO)$_3$(PH$_3$)], although the presence of the phosphine makes it closer to the phosphine adducts, but with longer Mn−P distances: $1.737 < d_{Mn-C(CO)} < 1.796$ Å, $1.168 < d_{C-O} < 1.177$ Å, and $2.786 < d_{Mn-P} < 3.946$ Å. Nevertheless, the transition state geometries are closer to the products, with relatively short Mn−P distances, exhibiting the same pseudo-octahedral geometry around the metal, and ligand X hapticipty found in the products. In other words, the greater part of the geometrical distortion associated with the haptotropic shift occurs before the transition state. Once this is reached, i.e., when the incoming phosphine is close enough, the uncoordinating X carbon atoms are already beyond bonding distances, $d_{Mn-C} > 2.5$ Å, and in the cases where a folded η^3-X is obtained (X = Ind, Chd, and Hnaph), most of this distortion is present in the transition state, as shown by the folding angles, Ω, only 7−8° lower than the values obtained for the phosphine adducts, [(η^3-X)Mn(CO)$_3$(PH$_3$)]. This seems to suggest that the haptotropic shift is the determining factor for the evolution of the reaction. The more easily the ligand X breaks two Mn−C(X) bonds (or three, in the case of Cp), the more facile will the transition state be reached, and the faster will be the reaction.

The energetics of the PH_3 addition to [(η^5-X)Mn(CO)$_3$] is compiled in Figure 4, for the five studied π ligands. Figure 4 values correspond to relative energies, the zero being taken as the reactants' total energy (PH_3 + [(η^5-X)Mn(CO)$_3$]), in each case. Thus, only the activation energies for the different cases can be related, a direct comparison between the transition state's stability being meaningless. Although not numerically comparable to the experimental values, due to the phosphine used in the calculations, the obtained activation energies, ΔE_a, allow the establishment of the following order of reaction rates: Cp ≪ Ind ≈ Chd < Flu < Hnaph, in absolute agreement with the available experimental data on the kinetics of the phosphine or phosphite addition to tricarbonylmanganese η^5 π ligand complexes. In fact, Basolo et al. found the reaction rate to be 10^8 times faster for the indenyl complex, when compared to the cyclopentadienyl analogue, and a 60-fold increase for the fluorenyl complex over the indenyl one.[2] On the other hand, recently published[65] kinetic studies for the P(OMe)$_3$ addition to [(η^5-Hnaph)Mn(CO)$_3$] showed the reaction to be over 10^6 times faster than for the indenyl species. We were not able to find any published experimental data for the cyclohexadienyl complex, but according to Figure 4 activation energies, the corresponding reaction rate should be comparable to the indenyl species. In other words, despite an expected increased stabilization of the indenyl transition state due to the benzene aromaticity gain, the corresponding activation energy is slightly higher (2 kcal mol^{-1}) than that calculated for the Chd reaction; this suggests that the reasons behind the different reaction rates should be traced to the initial [(η^5-X)Mn(CO)$_3$] reactants.

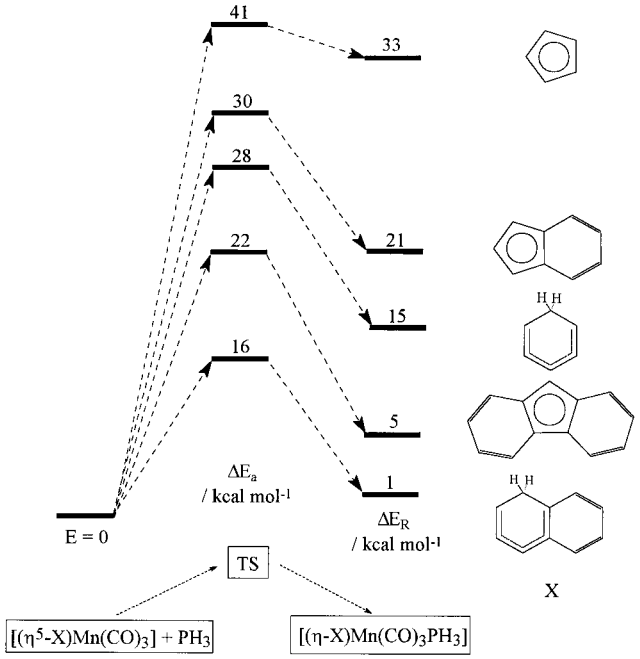

Figure 4. Relative energies (B3LYP/6-311+G**) for the PH_3 addition to [(η^5-X)Mn(CO)$_3$], X = Cp, Ind, Chd, Flu, and Hnaph.

Table 2. Comparison between the (η^5-X)−Mn Bond in the Reactants [(η^5-X)Mn(CO)$_3$]

X	⟨d_{M-C}⟩/Å (exp)	⟨d_{M-C}⟩/Å (theor)	OP{(η^5-X)$^-$−[Mn(CO)$_3$]$^+$}
Cp	2.138	2.162	0.629
Ind	2.162	2.178	0.544
Chd	2.176	2.174	0.506
Flu	2.192	2.194	0.483
Hnaph	2.209	2.217	0.426

The electronic structure and, particularly, the π ligand bonding to the metal in the η^5 complexes, the phosphine adducts, and the corresponding transition states were investigated to rationalize the order obtained for the reaction rates. In fact, some conclusions can be drawn from the comparison of the mean Mn−C distances for the five X carbon atoms bonded to the metal in all η^5 species, presented in Table 2 for both the experimental and the optimized structures. The previously discussed order for the reaction rate is maintained. Thus, Cp has the shortest Mn−C mean distance, followed by Ind, Chd, Flu, and, finally, Hnaph. These results seem to show a correlation between the (η^5-X)−Mn bond strength in the reactants, [(η^5-X)Mn(CO)$_3$], and the ease of the corresponding reaction.

Extended Hückel calculations were performed on [(η^5-X)Mn(CO)$_3$] model complexes with perfectly planar X

Scheme 4

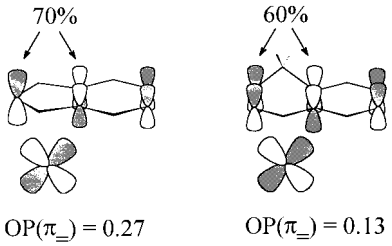

ligands and the same Mn−C distances, to understand the differences found for the (η^5-X)−Mn bond. In fact, an augmentation of the Mn−X distance can be caused by stereochemical reasons, or, on the other hand, it can be originated by electronic reasons, i.e., by an intrinsically weaker Mn−X bond. The values obtained for the $(\eta^5\text{-X})^-$−$[\text{Mn(CO)}_3]^+$ overlap populations (OP), compiled in Table 2, diminish along the same order: Cp < Ind ≈ Chd < Flu < Hnaph. In other words, there is a weakening of the π ligand bond to the metal in the η^5 complexes that justifies the elongation of the Mn−X distance and follows the same order as the increase of the reaction rate.

The weakening of the (η^5-X)−M bond strength with the increase of the π system extension for the ligands coordinating through a C_5 pentagon (Cp, Ind, and Flu) was formerly studied,[54] being related to the fraction of the ligand atoms directly bonded to the metal. Thus, the larger the ligand, the smaller will be the fraction corresponding to the five atoms connected to the metal in an η^5 coordination mode, and the smaller will be the fraction of the electronic density on the ligand's orbitals (π_σ, $\pi_{||}$, and $\pi_\perp$) effectively involved in the interaction, resulting in a weaker bond. The same reasoning holds for the comparison between Chd and Hnaph. On the other hand, the comparison between Cp and Chd, or Ind and Hnaph (see Table 2), indicates that the geometry of a C_5 pentagon yields a better overlap between the orbitals of the interacting fragments and produces a stronger bond than the one achieved through five carbon atoms of a C_6 ring. The final (η^5-X)−Mn bond results from the summation of those two effects. This is illustrated, for example, in the comparison of the $\pi_{||}$ interaction for the polyenyl bond in the indenyl and 1-hydronaphthalene η^5 complexes (Scheme 4). The overlap population between the intervening fragment orbitals doubles going from Hnaph (OP($\pi_{||}$) = 0.13) to Ind (OP($\pi_{||}$) = 0.27), partly due to the better overlap achieved with the indenyl coordination geometry and partly to a greater portion of the ligand $\pi_{||}$ orbital electronic density on the atoms connected to the metal: 70% for Ind vs 60% for Hnaph.

The reaction rate for the phosphine addition to [(η^5-X)Mn(CO)_3] complexes seems to correlate with the polyenyl bond strength, (η^5-X)−Mn, on the η^5 reactants. In fact, the π ligand haptotropic shift associated with the reaction is the key factor with respect to the reaction ease, as shown by transition states close to the products; that is, the coordination geometry and hapticipty of the ligands X in the transition state are practically those observed in the phosphine adducts, [(η-X)$\text{Mn(CO)}_3(\text{PH}_3)$]. Thus, once the geometrical distortion corresponding to the haptotropic shift, or ring slippage, is reached, the reaction proceeds easily toward the product. In other words, the reaction rate depends directly on the ease of the breaking of two (or three, in the case of Cp) Mn−C(X) bonds, out of the five present in the η^5 complexes. Hence, stronger (η^5-X)−Mn bonds will lead to more difficult haptotropic shifts and, consequently, to slower reactions, or even to no reaction at all, as in the case of Cp.[2] This same result was previously suggested by a calorimetric study of molybdenum and tungsten complexes with Cp and Ind ligands, showing the latter to be more weakly bonded to the metal (by 10−15 kcal/mol) and leading to the conclusion that ground state thermodynamic differences may be the basis of the indenyl effect.[77]

The same reasoning explains the different stability of the phosphine adducts relative to the corresponding reactants (ΔE_R in Figure 4). A stronger X−Mn bond in the η^5 complexes will produce an enhanced stability of the corresponding [(η^5-X)Mn(CO)_3] species and, thus, a comparatively less stable ring slipped product. Cp has the more destabilized product, [(η^2-Cp)$\text{Mn(CO)}_3(\text{PH}_3)$], 33 kcal mol^{-1} above the reactants and only 8 kcal mol^{-1} from the transition state; on the other hand, the Hnaph product, [(η^3-Hnaph)$\text{Mn(CO)}_3(\text{PH}_3)$], has an energy similar to the corresponding reactants, being 15 kcal mol^{-1} away from the transition state. Therefore, it is not surprising that the latter complex is the only one of the five here studied with an X-ray crystal structure determination on a related complex.[65]

Conclusions

All the adducts resulting from a phosphine addition to [(η^5-X)Mn(CO)_3] complexes present shifted π ligands, X, resulting from the stabilization of a Mn−X antibonding orbital ($\pi_{||}$*), occupied as a consequence of the two-electron increase on the metal center. In the indenyl, cyclohexadienyl, and 1-hydronaphthalene species, [(η^3-X)$\text{Mn(CO)}_3(\text{PH}_3)$], that stabilization is achieved through ring-folded polyenyl ligands, with the coordination geometry well-known for indenyl η^3 complexes, and significant folding angles, 24° < Ω < 40°. The fluorenyl ligand adopts an exocyclic allylic coordination mode on the phosphine complex, as the two fused benzene rings prevent the folding of the C_5 pentagon. Ring slippage of the cyclopentadienyl ligand is found on the corresponding complex, ending up with an η^2 coordinated planar Cp, due to the destabilization associated with the folding of this ligand.

In all the transition states the X hapticipty and the coordination geometry in the metal sphere are similar to those of the corresponding phosphine products. This indicates that the haptotropic shift of the π ligand, X, is the key factor for the reaction rate, since once that distortion is completed, the products, [(η-X)$\text{Mn(CO)}_3(\text{PH}_3)$], will be easily reached.

The obtained order of reaction rates, Cp ≪ Ind ≈ Chd < Flu < Hnaph, is in absolute agreement with the experimental kinetic data, available for all ligands but cyclohexadienyl, and suggests that this ligand complex, [(η^5-Chd)Mn(CO)_3], should present a reaction rate comparable with the indenyl analogue. A correlation was found for the (η^5-X)−Mn bond strength in the reactants

(77) Kubas, G. J.; Kiss, G.; Hoff, C. D. *Organometallics* **1991**, *10*, 2870.

and the ease of the reaction. In fact, the weaker the Mn−X bond, the easier is the breaking of the two (or three, in the case of Cp) Mn−C bonds, corresponding to the haptotropic shift. This leads to a more facile reaching of the transition state and, consequently, a faster reaction.

Computational Details

The geometry optimizations were accomplished by means of ab initio and DFT calculations performed with the Gaussian 98 program.[78] The B3LYP hybrid functional with a 3-21G(*) basis set[79] was used in all optimizations. This functional includes a mixture of Hartree−Fock[67] exchange with DFT[68] exchange−correlation, given by Becke's three-parameter functional[80] with the Lee, Yang, and Parr correlation functional, which includes both local and nonlocal terms.[81,82] All the optimized geometries are the result of full optimizations without any symmetry constrains. Single-point calculations were run on the optimized structures at the same theory level and a 6-311+G** basis set.[83]

Transition state optimizations were performed with the Synchronous Transit-Guided Quasi-Newton Method (STQN) developed by Schlegel et al.[84] The transition state determinations were confirmed by frequency calculations yielding one imaginary frequency, as well as small displacements along the reaction path in both directions yielding the reactants and the products, respectively.

The extended Hückel calculations[69,70] were done with the CACAO program[85] and modified H_{ij} values were used.[86] The basis set for the metal atoms consisted of *n*s, *n*p, and (*n*−1)d orbitals. The s and p orbitals were described by single Slater-type wave functions, and the d orbitals were taken as contracted linear combinations of two Slater-type wave functions. Only s and p orbitals were considered for P. The parameters used for Mn were the following (H_{ii} (eV), ζ): 4s −9.880, 1.800; 4p −5.450, 1.800; 3d −12.530, 5.150, 1.900 (ζ_2), 0.5311 (C_1), 0.6479 (C_2). Standard parameters were used for other atoms. Calculations were performed on models based on the optimized geometries with idealized maximum symmetry and the following distances (Å): Mn−C (polyenyl) 2.20, Mn−C (CO) 1.80, Mn−P 2.30, C−O 1.15, C−C 1.40, P−H 1.40, C−H 1−08; and angles (deg): X−Mn−CO 120 ([(η^5-X)Mn(CO)$_3$] complexes), CO(eq)−Mn−CO(eq) 105, P−Mn−CO(ax) 170 ([(η^3-X)Mn(CO)$_3$(PH$_3$)] complexes).

Acknowledgment. The author gratefully thanks Dr. José Carlos Pereira for the granting of computational resources. Praxis XXI is acknowledged for partial funding of this work.

Supporting Information Available: Tables of atomic coordinates for all the optimized structures. This material is available free of charge via the Internet at http://pubs.acs.org.

OM000195J

(78) Frisch, M. J.; Trucks, G. W.; Schlegel, H. B.; Scuseria, G. E.; Robb, M. A.; Cheeseman, J. R.; Zakrzewski, V. G.; Montgomery, J. A., Jr.; Stratmann, R. E.; Burant, J. C.; Dapprich, S.; Millam, J. M.; Daniels, A. D.; Kudin, K. N.; Strain, M. C.; Farkas, O.; Tomasi, J.; Barone, V.; Cossi, M.; Cammi, R.; Mennucci, B.; Pomelli, C.; Adamo, C.; Clifford, S.; Ochterski, J.; Petersson, G. A.; Ayala, P. Y.; Cui, Q.; Morokuma, K.; Malick, D. K.; Rabuck, A. D.; Raghavachari, K.; Foresman, J. B.; Cioslowski, J.; Ortiz, J. V.; Stefanov, B. B.; Liu, G.; Liashenko, A.; Piskorz, P.; Komaromi, I.; Gomperts, R.; Martin, R. L.; Fox, D. J.; Keith, T.; Al-Laham, M. A.; Peng, C. Y.; Nanayakkara, A.; Gonzalez, C.; Challacombe, M.; Gill, P. M. W.; Johnson, B.; Chen, W.; Wong, M. W.; Andres, J. L.; Gonzalez, C.; Head-Gordon, M.; Replogle, E. S.; Pople, J. A. *Gaussian 98*, Revision A.6; Gaussian, Inc.: Pittsburgh, PA, 1998.

(79) (a) Binkley, J. S.; Pople, J. A.; Hehre, W. J. *J. Am. Chem. Soc.* **1980**, *102*, 939. (b) Gordon, M. S.; Binkley, J. S.; Pople, J. A.; Pietro, W. J.; Hehre, W. J. *J. Am. Chem. Soc.* **1982**, *10*, 2797. (c) Pietro, W. J.; Francl, M. M.; Hehre, W. J.; Defrees, D. J.; Pople, J. A.; Binkley, J. S. *J. Am. Chem. Soc.* **1982**, *104*, 5039. (c) Dobbs, K. D.; Hehre, W. J. *J. Comput. Chem.* **1986**, *7*, 359. (d) Dobbs, K. D.; Hehre, W. J. *J. Comput. Chem.* **1987**, *8*, 861. (e) Dobbs, K. D.; Hehre, W. J. *J. Comput. Chem.* **1987**, *8*, 880.

(80) Becke, A. D. *J. Chem. Phys.* **1993**, *98*, 5648.

(81) Lee, C.; Yang, W.; Parr, R. G. *Phys. Rev. B* **1988**, *37*, 785.

(82) Miehlich, B.; Savin, A.; Stoll, H.; Preuss, H. *Chem. Phys. Lett.* **1989**, *157*, 200.

(83) (a) McClean, A. D.; Chandler, G. S. *J. Chem. Phys.* **1980**, *72*, 5639. (b) Krishnan, R.; Binkley, J. S.; Seeger, R.; Pople, J. A. *J. Chem. Phys.* **1980**, *72*, 650. (c) Wachters, A. J. H. *J. Chem. Phys.* **1970**, *52*, 1033. (d) Hay, P. J. *J. Chem. Phys.* **1977**, *66*, 4377. (e) Raghavachari, K.; Trucks, G. W. *J. Chem. Phys.* **1989**, *91*, 1062. (f) Binning, R. C.; Curtiss, L. A. *J. Comput. Chem.* **1995**, *103*, 6104. (g) McGrath, M. P.; Radom, L. *J. Chem. Phys.* **1991**, *94*, 511.

(84) (a) Peng, C.; Ayala, P. Y.; Schlegel, H. B.; Frisch, M. J. *J. Comput. Chem.* **1996**, *17*, 49. (b) Peng, C.; Schlegel, H. B. *Isr. J. Chem.* **1994**, *33*, 449.

(85) Mealli, C.; Proserpio, D. M. *J. Chem. Educ.* **1990**, *67*, 39.

(86) Ammeter, J. H.; Bürgi, H.-J.; Thibeault, J. C.; Hoffmann, R. *J. Am. Chem. Soc.* **1978**, *100*, 3686.